# Phytolith assemblages in the leaves of *Guadua* bamboo in Amazonia

**Risto Kalliola[1*]. Ari Linna[1]. Linnea Toiviainen[1]. Kalle Ruokolainen[2]**

Received: 28 June 2019/Accepted:17 August 2019


**Abstract**: We studied phytoliths (plant stones) from 228 leaf samples of *Guadua weberbaueri* and *Guadua sarcocarpa* bamboos from eleven collection locations in Southern Peruvian Amazonia and in the state of Acre in Brazil. Four leaf-blade transverse thin sections were made by grinding and smoothing them into a 30 µm thickness, and over 550 phytolith slides created by using both the dry ashing and wet oxidation methods. Large-sized (up to 50 µm) cuneiform bulliform cells in the intercostal adaxial leaf-blade areas were the most conspicuous phytoliths in *Guadua* leaves, but their abundance varied even locally. Other recurrent phytolith types included bilobate, saddle, and rondel shaped short cells; long cells in many different sizes and ornamentations; and prickle hairs, spikes, stomatal, and inter-stomatal cells. We found the definite classification of phytoliths into morphotypes difficult because of their variable sizes, forms, and surface characteristics. Conjoined tricellular cell structures with one to three mineral-accumulating cells forming a characteristic mushroom-like constellation were also documented. Fusoid cells forming dense rows attached to the costal zones locally showed mineralization, indicating their role in inorganic mineral mobilization and deposition in *Guadua* leaves. Foliar phytolith assemblages showed little variation among the different collection locations compared to the variation found among leaves within individual sites.

*Keywords*: Amazonia, bamboo, fusoid cell, *Guadua*, leaf, phytolith

*Corresponding Author

[1] Department of Geography and Geology, University of Turku, FI20014 Turku, Finland

[2] Department of Biology, University of Turku, FI20014 Turku, Finland
E-mail: risto.kalliola@utu.fi

Published online 21 October 2020

## Introduction

The subfamily of Bambusoideae (Poaceae) inhabits a wide range of tropical and subtropical habitats. Bamboos absorb silicon from the soil solution and deposit it as amorphous hydrated silicon ($SiO_2.nH_2O$) in the cell wall, cell lumina, and intercellular spaces of various tissues (Piperno, 2006). These phytoliths (plant opals, plant stones) can be both abundant and morphologically diverse, and diagnostic up to the level of tribe or genus. Phytoliths are preserved in the soil even after the organic parts of the plant have degraded, making them useful as microfossils to help paleoecological and archaeological studies (Ball *et al*., 2016; Watling *et al*., 2015). Moreover, phytoliths often occlude carbon (PhytOC), which is preserved in the soil and contribute to carbon sequestration (Parr *et al*., 2010).

Probably the world's largest lowland bamboo forests in their natural state are located in south western Amazonia in Brazil and Peru, where two species of arborescent semi-scandent bamboos (*Guadua weberbaueri* Pilg. and *Guadua sarcocarpa* Londono and Peterson) dominate tropical rain forests in an area of over 160,000 km$^2$ (de Carvalho *et al*., 2013). These bamboo species form large patches that flower gregariously and die off after the flowering event'(Nelson, 1994). It has been argued that the pre-Colombian civilization that occupied at least a part of these present-day bamboo forests utilised the die-off events as a window of opportunity to clear the forest using the fires fuelled by dead bamboo biomass. Hence, *Guadua*

phytoliths in archaeological deposits are among the key microfossils of that region (McMichael *et al.*, 2013; Watling *et al*., 2016).

The relevance of *Guadua* phytoliths in archaeology and their potential contributions to carbon sequestration call for a closer look to examine their characteristics in the living plant. Opal phytoliths in grasses can be variable, depending on when, where, and how silicon deposition occurs in the plant. Phytoliths with bulliform morphology are common in the family, but many other phytolith morphotypes have also been described (Rapp and Mulholland, 1992). In the *Guadua* bamboos, known morphotypes include bulliform, bilobate, saddle, rondel, cross and narrow elliptate phytoliths (Piperno and Pearsall, 1998; Watling *et al*., 2016). However, the phytolith composition of a given plant species can vary from one individual plant to another (Twiss *et al*., 1969). Variations also occur between different parts of a single leaf blade, between the leaves of an individual plant, and among different plant structures. For example, in the bamboo genus Aristida, rondels occur in both the leaves and inflorescences, whereas saddles form in the leaves, culms, and inflorescences (Piperno and Pearsall, 1998). Moreover, individual plants growing in different habitats may differ in their phytolith compositions (Twiss *et al*., 1969).

As such, there are no studies that describe the variation in appearance of foliar *Guadua* bamboo phytoliths between individuals or populations. The study aims to fill this gap by describing the *Guadua* phytoliths in leaves sampled widely from eleven different locations across the Amazonian bamboo forest area. By using a variety of analytical methods, we attempt to answer the following research questions: (1) Which kinds of phytoliths do the living *Guadua* bamboo leaves contain? (2) Where do the different phytolith types occur in the leaf structure? (3) How much do the overall phytolith assemblages vary among different individuals or populations?

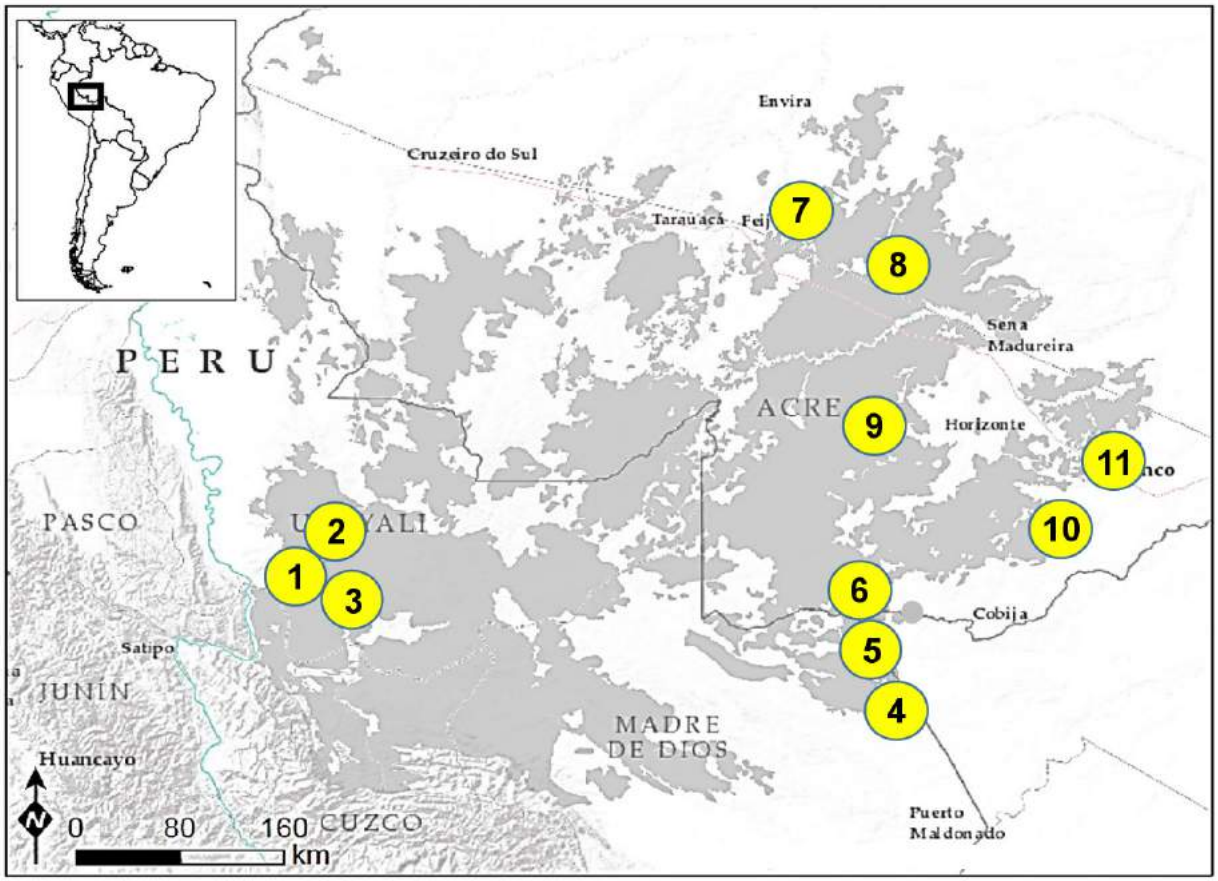


**Fig 1.** The bamboo sampling locations in the lowland Amazonia. The grey shaded area shows the total distribution of the bamboo forest formation according to de Carvaljo *et al.,* (2013). 1 = San Carlos, 2 = Ojeayo, 3 = Cumarillo, 4 = Tahuamanu, 5 = Primavera. 6 = Chico Mendes, 7 = Maciopira, 8 = Edmilson, 9 = São Tomé, 10 = Campo Alegre, 11 = Ivo.

## Materials and methods

The *Guadua* samples were collected during 2017 and 2018 from eleven different locations in Southern Peruvian Amazonia and the Brazilian state of Acre (Fig. 1). The Brazilian samples were on average fewer than those collected from Peru (Table 1). Due to difficulty in distinguishing *G.sarcocarpa* from *G. weberbaueri* in sterile conditions, the common term *Guadua* bamboo is used throughout the text, acknowledging the possibility that our material could represent two different species (Olivier and Poncy, 2009).

In each location, the regional abundance of bamboo-dominated forests was confirmed by examining Landsat TM satellite images wherein these forests are clearly discernible due to their high reflectance in the near-infrared radiation. The targeted bamboo stands in the patches were identified with the help of local inhabitants. All the collection locations were below 200 meters above sea level. Annual rainfall in these locations varies between 2000 and 2500 mm per year, and there is a distinct dry season, which typically lasts three to four months. *Guadua* leaves are commonly ca. 20 cm long and 2 to 3 cm wide. Foliar samples (about 5 cm long) from the central parts of leaves were used for the study, and in total, 228 different leaf blades were collected from 7 to 41 bamboo ramets in each location, with the highest numbers of collections made in the Peruvian locations (Table 1). Each leaf sample was taken at a minimum of 30 m apart from another collected culm, so as to represent separate genets. The samples were assigned-consecutive collection numbers from 1 onwards in each location. Care was taken to sample leaves that were healthy-looking. The collected samples were folded, placed in small paper bags, and immediately deposited in silica gel to achieve rapid drying.

The laboratory studies were undertaken in the geoscientific laboratory at the University of Turku, Finland. Three different analytical lineages used to produce microscopy slides are shown in Fig 2. Foliar transverse thin sections were prepared from four leaf-blade samples. Because phytoliths are minerals, thin section methodology used in mineralogy and petrology was applied. Air-dried leaf-blade samples were first embedded into Struers EpoFix and air bubbles were removed via a low-pressure treatment (200 mbar) for about 20 minutes. After the samples had hardened at room temperature for several days, they were levelled at the broadest point of the leaf using an Astera Solutions precision grinding machine GRN16 (#400 diamond cup wheel) and then attached with EPOTEK 301 into levelled glass that had also been produced using the GRN16 (#140). The samples were cut with an Astera Solutions precision cut-

**Table 1.** Collection locations with their respective numbers of studied *Guadua* leaves, transverse section microscopy samples and dry ashing photographs.

| Location | Country | Leaves studied | Transverse sections | Dry ashing photographs |
|---|---|---|---|---|
| San Carlos | Peru | 32 | 1 | 97 |
| Ojeayo | Peru | 26 | 2 | 82 |
| Cumarillo | Peru | 41 | 0 | 102 |
| Tahuamanu | Peru | 38 | 0 | 96 |
| Primavera | Peru | 36 | 1 | 88 |
| Chico Mendes | Brazil | 10 | 0 | 16 |
| Maciopira | Brazil | 7 | 0 | 10 |
| Edmilson | Brazil | 11 | 0 | 15 |
| Sao Tomé | Brazil | 10 | 0 | 15 |
| Campo Alegre | Brazil | 10 | 0 | 23 |
| Ivo | Brazil | 7 | 0 | 13 |
| Total | | 228 | 4 | 557 |

off saw CUT8 and levelled down to 30 µm using the GRN16 (#800). The samples were finalised by diamond polishing with Saint-Gobain W606AS slurries and Struers Largo (3 micron), PoliSat1 (1 micron) and PoliFloc4 (1/4 micron) polishing pads.

In the second lineage, phytolith spodograms were prepared with the dry ashing method (Piperno, 2006: 97). This method allows for observing phytoliths in their original places in the plant tissue. The bamboo samples were placed between two microscope slides and then heated in the laboratory furnace by gradually increasing the temperature 50° C every 10 minutes, to 600° C. A lower maximum temperature was tested, but abandoned, as the burning remained incomplete. After the samples had cooled, the spodograms were finalised by removing the cover slide, the sample mounted using EPO-TEK 301 epoxy, and the sample slide covered with a glass cover.

The third methodological lineage was wet oxidation (Piperno, 2006: 97; Katz *et al*., 2010) to allow individual phytolith examination and photography. The bamboo leaves were first soaked in a 1% solution of Alconox detergent and then washed with distilled water. The organic materials were removed using nitric acid ($HNO_3$) in a bath of boiling water by adding pinches of solid potassium chlorate ($KClO_3$) to speed up the reaction time. Finally, the samples were washed with distilled water and centrifuged for 10 minutes at 1500 rpm in suspension with sodium polytungstate (density 2.4 $gml^{-1}$). The resulting concentrated phytolith suspension was then dried and epoxy-mounted on microscopy slides.

Transmitted light microscopy with polarised light in magnifications of 25X, 100X, 250X, and 400X was used to examine and photograph the microscope slides to find and describe morphologically distinctive phytolith types. The crossed Nicols illu-

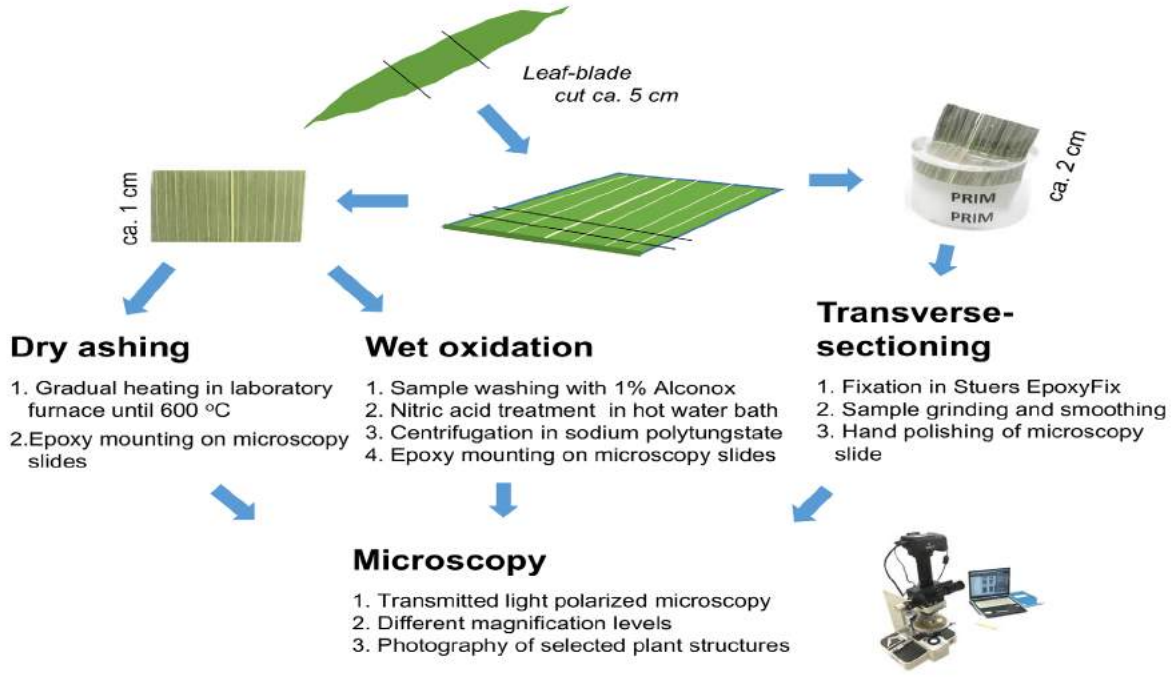


**Fig 2.** Overview of the three methodological lineages used for producing microscope slides of *Guadua* foliar phytoliths.

mination method was applied, revealing samples' optical interference effects (Kurosu *et al*., 1973). The leaf-blade slides were examined by having both the adaxial and abaxial sides facing up in order to observe all the relevant characteristics. The International Code for Phytolith Nomenclature (Madella *et al*., 2005) was used as a guide for the phytolith classification.

The proportional abundances of the most recurrent phytolith morphotypes in the different collection locations were examined and estimates were made by the same person (LT) to avoid human bias. For each of the collected leaf, 2 to 5 microscopy slides were examined with the relative abundancy estimate scale proposed by Twiss *et al*., (1969): "rare" (only a couple of grains of this morphological class in the leaf sample), "common" (several grains) and "abundant" (high grain density). The value zero was assigned to absence and values 1, 2 and 3 to each of the abundance classes, respectively. These numerically expressed abundance estimates were used to compute a principal components analysis (PCA) of the 228 leaves. The PCA was calculated from a covariance matrix, effectively meaning that those phytolith types presenting most variation in abundance classes also got the most weight in the PCA.

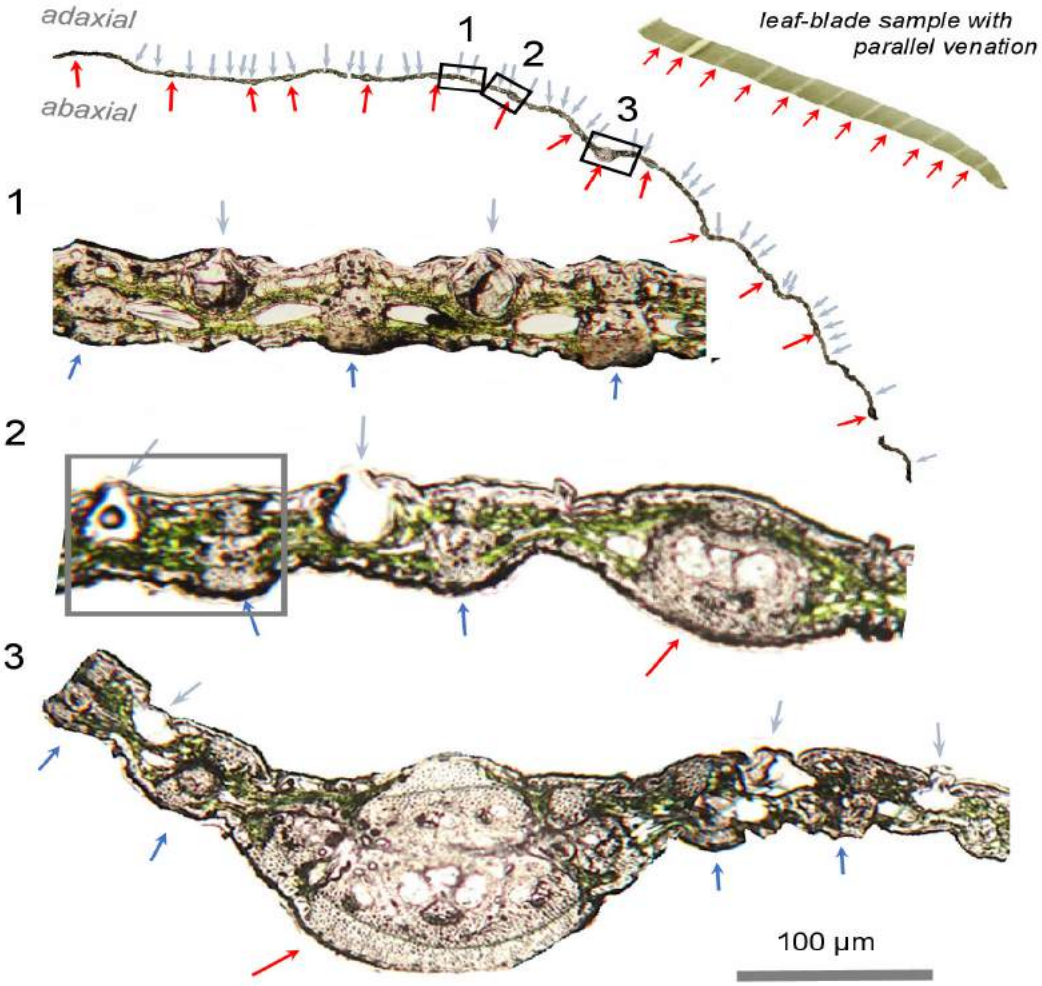


**Fig 3.** Foliar transverse sections of *Guadua* bamboo (Primavera 10). Grey arrows in the adaxial side show the locations of cuneiform bulliform cells. Red arrows in the abaxial side show the vascular bundles with xylem and phloem. In the three magnified sections, photosynthetic mesophyll is green, and minor-sized sclerenchyma bundles are marked with blue arrows. The grey square with a bulliform cell and vein (sclerenchyma bundle) is magnified in Fig. 4a.

## Results

The studied *Guadua* leaves were 50-80 µm thick with yellowish costal zones (veins) and darker coloured intercostal areas with photosynthetic chlorenchyma tissue (Fig. 3). Leaves generally showed similar structures in all transverse sections, yet their detailed characteristics varied (Table 2). Densities of vascular bundles and bulliform cells were the highest in the sample from Primavera. Minor veins without xylem and phloem tissues formed further costal zones as sclerenchyma bundles. Bulliform cells were conspicuous in the adaxial intercostal areas (Fig. 3b and 4a). The inner leaf structure also included fusoid cells attaching on both sides of the bundles. The inside materials of fusoid cells and bulliform cells appeared equal when different sample illumination methods were used (Fig.4b).

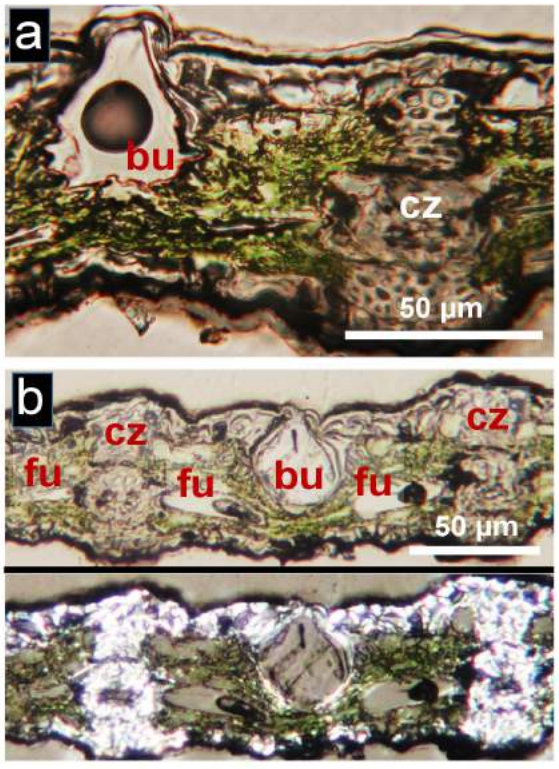


**Fig 4.** Detailed foliar transverse sections of *Guadua* bamboo (Primavera 10). (a) A cuneiform bulliform cell (bu) with a roundish bubble like cavity inside, and a costal zone (cz) consisting of a sclerenchyma bundle (vein). (b) A cuneiform bulliform cell, two costal zones (cz) and fusoid cells (fu) attached to them. The image shows the same area in transmitted light microscopy with one Nicol (above) and crossed Nicols (below).

Morphological phytolith classification in the dry ashing and wet oxidation microscopy slides was sometimes problematic because of the varying sizes, shapes, and surface ornamentations of the phytolith grains (Fig 5). The following descriptions characterise the most recurrent phytolith morphotypes and consider their anatomical positions in the leaf-blade structure.

Bulliform cells were clearly the most conspicuous category in most leaves due to their commonness and large size (40-80 µm). Cell morphology and appearance as well as their degree of mineralization varied between the studied microscopy slides. In side view of the samples prepared by transverse sectioning (Fig. 3 and 4) or wet oxidation (Fig. 5a), bulliform cells were found to be cuneiform and occured with different densities (Table 2) in the adaxial epidermis, with their thickest parts extending deep in the leaf blade structure. In the top view, in turn, bulliform cells were parallelepipedal (Fig. 5b) and formed chain-like lines in the intercostal zone, particularly eye-catching when most of the cells were mineralised (Fig. 6a). In a more detailed view, bulliform cells can show explicit morphologies such as somewhat scaly structure or having some sort of internal structure.

Short cells ranging from ca. 10 µm to ca. 30 µm showed distinctive morphological flexibility as a transition from cells with characteristically bilobate or saddle-shaped form (Fig. 5c-f and Fig. 6 b-e) to rondels (Fig. 5g) and cross-shaped (scarce morphotype) cells (Fig. 5h). Their forms also varied from almost symmetric to asymmetric. For these reasons, it was often difficult to define the definite morphotype of a given cell. Bilobate and saddle-shaped cells typically occured in between long cells (see Fig. 5d) and had a near-perpendicular position against the leaf-blade length (Fig. 6). Short cells were in general bigger in the costal zone compared to the intercostal zone. All short cell types had smooth outlines without specific ornamentations, and held a dark spot (sometimes two) at either end of the cell interior.

Long cells constituted another heterogeneous category as their sizes, forms and detailed ornamentations varied considerably. In many cases long

**Table 2.** Foliar characteristics in the transverse sections of four studied specimens. Densities are for 10 mm of leaf width.

| Location | Width of studied leaf-blade as mm | Density of vascular bundles | Density of bulliform cells |
|---|---|---|---|
| Primavera 10 | 25 | 6.0 | 14.0 |
| Ojeayo 5 | 34 | 2.4 | 2.6 |
| Ojeayo 20 | 26 | 2.3 | 3.8 |
| San Carlos 7 | 19 | 4.2 | 1.0 |

cells were only visible for their outlines but not as phytoliths with internal mineralization (Fig. 5d). At places, however, individual long cells showed apparent mineral accumulation (Fig. 6c). Long cell phytoliths were found to be elongate papillate, echinate, or trapeziform with their lengths varying between 20 µm and 60 µm (see Fig. 5i-m). We considered cells with particularly strong surface ornamentation to be elongated grass cells (Fig. 5i and k) but did not apply more detailed long cell classification to definite phytolith morphotypes. Long cell phytoliths were found to never hold dark spots inside.

Prickle hairs, which can be bi- or tricellular constructions, attach via a relatively thick base to the intercostal zone, especially in the adaxial epidermis (Fig. 5n and o). Their lengths varied a lot, from about 20 µm to at least 100 µm. The intercostal zone also contained another characteristic cell construction with occasional mineralization. We herein name these conjoined tricellular combinations as "mushroom composites" for their appearance, which resembles the *Boletus* mushroom (Fig. 5p). Their base is oval-shaped, the middle cell is a small square, and the distal cell is the largest, having a gavel-like shape. Mineralization was found in some only or in all of these cells. The base cell and the distal cell were found to hold a dark spot inside. Also in the dry ashing samples, stomatal guardian cells and interstomatal short cells were often visible for their outlines but also showed partial or full mineralization (Fig. 5s and t). Spike-like prickle hairs with partial internal mineralization were found to occur at the leaf margin areas of some samples (Fig. 5q) and an instance of a globular echinate phytolith was also observed in the samples (Fig. 5r).

Fusoid-shaped cells that were 30-50 µm long and ca. 5 µm wide were found attached to the leaf veins (Fig. 4) in many dry ashing spodograms (Fig. 6d-f). Arranged in dense rows nearly perpendicular to the veins, they occured as fusiform translucent cavities or contained dark mineralization. The degree of mineralization varied between the different leaf samples. A few instances of mineralization with similar appearance was also observed inside the veins (Fig. 6e), in cases extending to the intercostal areas. However such fusoid shaped structures were found absent in the samples prepared by wet oxidation.

Phytolith assemblages did not show evident dissimilarities among the eleven study locations (Table 3, Figure 7). Bulliform cells, bilobate to saddle cells and fusoid cells were found in almost all samples with their prevalence in the microscopy slides at 86%, 89% and 83%, respectively. In the majority of samples their relative abundances could be classified as common or abundant. Rondels had an overall prevalence of only 7%, being particularly few in the Brazilian samples. Long cell phytoliths were prevalent in most Peruvian locations with their highest relative abundances at Primavera and Cumarillo. Brazilian locations, in turn, showed more commonly elongated grass cells. Prickle hairs were recurrent in most locations (prevalence 57%) but with variable abundances. "Mushroom composites" formed phytoliths only in rare occasions and their prevalence was low with exception of Maciopira (43%).

The result of the PCA (Fig. 7b) suggests that the variation in the foliar phytolith spectrum can be almost as large within a site or population as it is

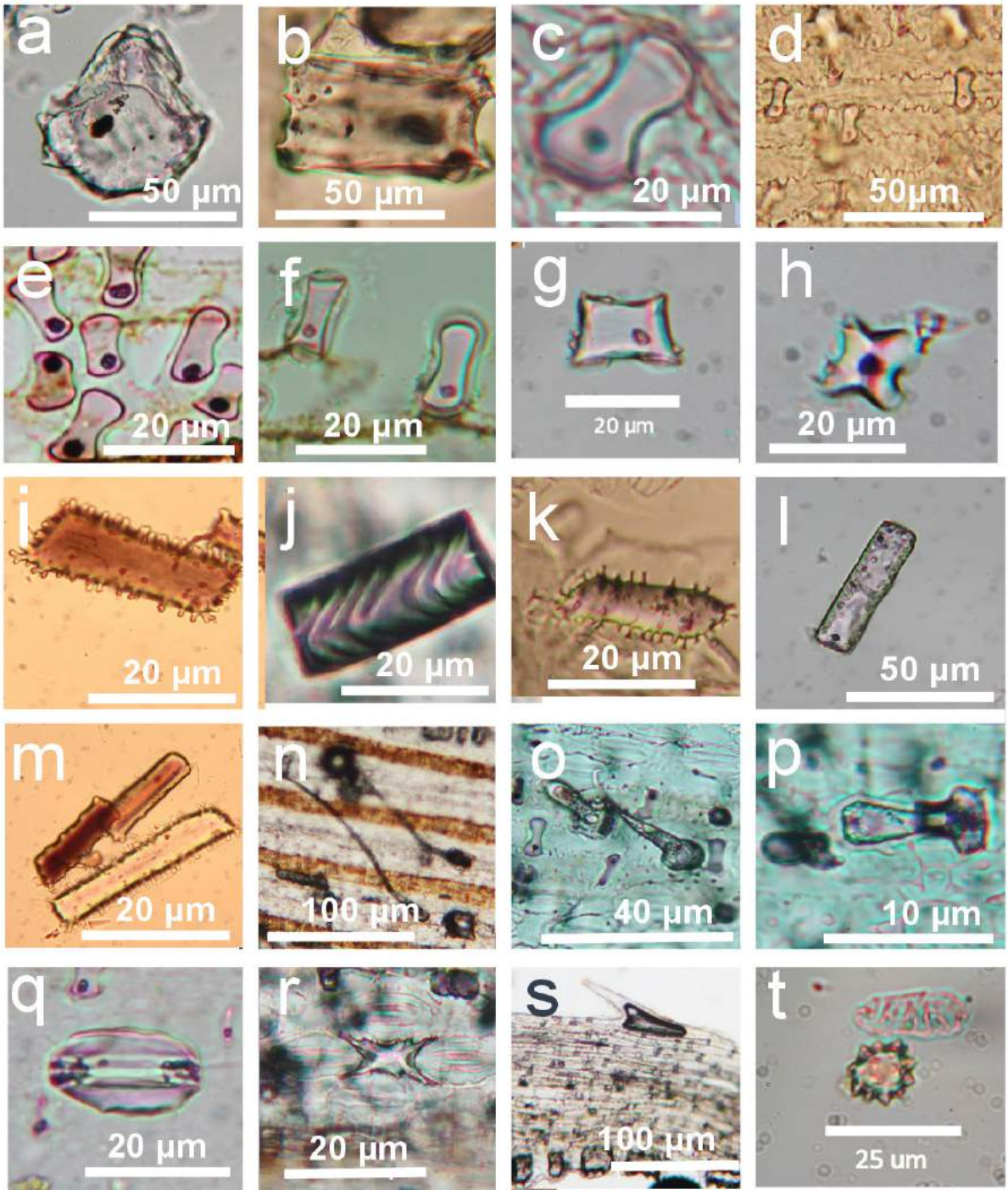


**Fig 5.** Phytolith morphotypes found in *Guadua* leaf blades in Amazonia. (a) cuneiform bulliform cell side view; (b) parallelepiped bulliform cell top view; (c) bilobate to saddle shaped short cells (d-e); (f) rondel (left) and bilobate or saddle shaped short cells; (g) rondel; (h) cross-shaped short cell; (i-m) different kinds of long cells; (n) and (o) prickle hair cells (probably bicellular); (p) tricellular "mushroom composite" with enlarged base; (q) stomatal guardian cells with different levels of mineralization; (r) mineralised inter-stomatal short cell; (s) silicified unicellular prickle hair; (t) globular echinate short cell;. Pictures g, h, l, n, q, r, s, and t came from dry ashing and the rest from the wet oxidation method.

among sites. No obvious separation was visible among sites but there was a slight tendency of three of the Brazilian sites (Campo Alegre, Ivo and São Tomé) to appear more on the left side of the ordination than the rest of the sites. This implies that the studied phytolith assemblages were nearly but not fully identical among the different study sites.

## Discussion

*Guadua* bamboo leaves from the lowland Amazonia show widespread mineralization – probably predominantly silica accumulation – in their bulliform cells and various morphotypes of short cells and long cells. Other cell types with occasional mineralization include stomatal guardian cells, interstomatal short cells, prickle hairs, the tricellular assembly called a "mushroom composite" and fusoid cells. Globular echinate cells (Fig. 5t) occurred in only one of the several hundred microscopy slides and is hence attributed to a likely sample contamination.

The PCA did not demonstrate any obvious differences in foliar phytolith assemblages among our sampling locations. Three Brazilian sites (São

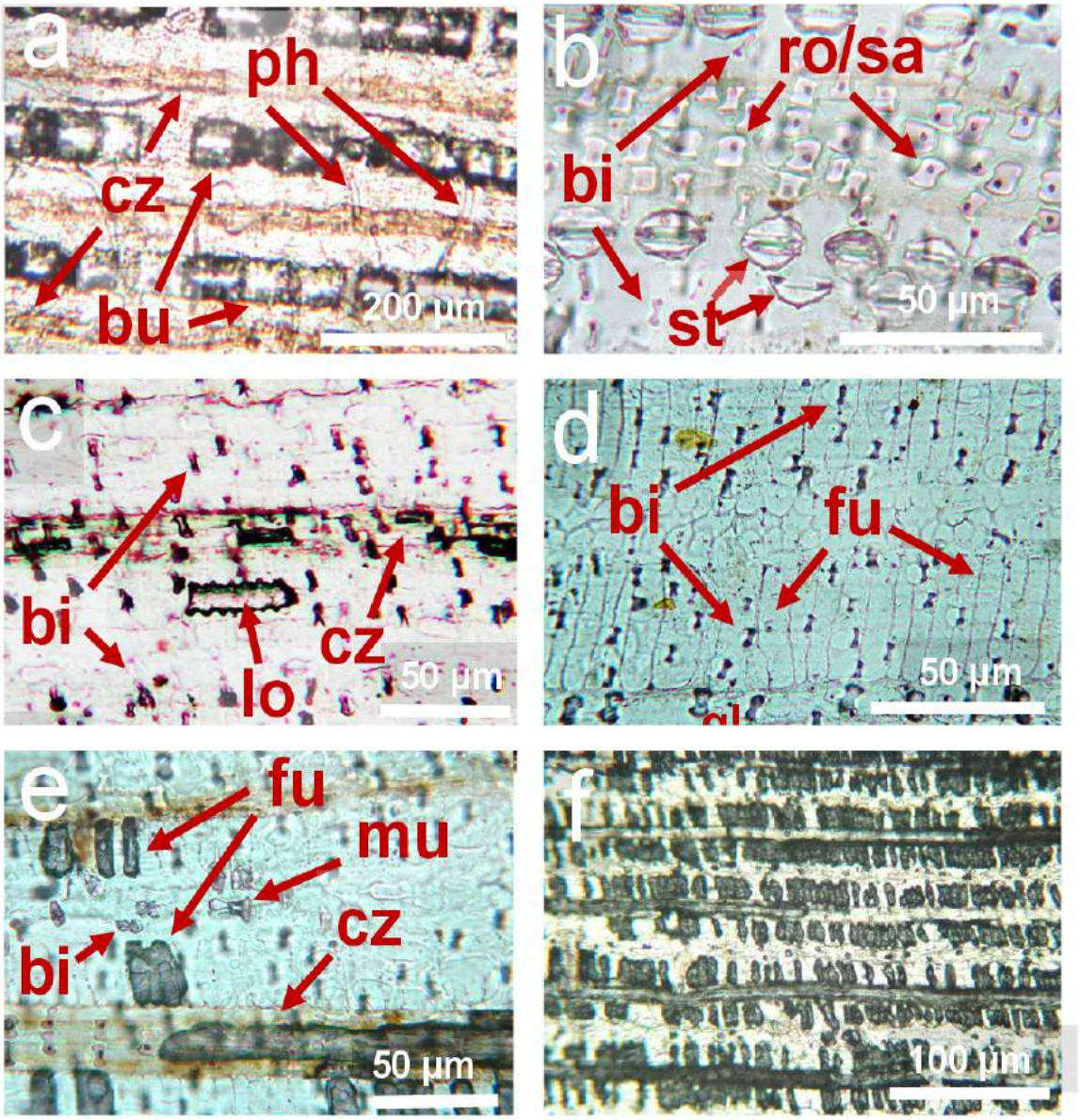


**Fig 6.** Anatomical phytolith occurrences in dry ash-imaging in *Guadua* leaf-blades. (a) rows of bulliform cells (bu), solitary prickle hairs (ph) and three costal zones (cz); (b) bilobate (bi) and rondel (ro) or saddle (sa) shaped short cells, and stoma cells (st) with different degrees of mineralization; (c) lone mineralised long cell (lo) with plentiful bilobate short cells and a costal zone; (d) translucent fusoid cells (fu) and numerous bilobate cells in different sizes (picture is of the abaxial side of the leaf); (e) fusoid cells (both having and not having internal mineralization), costal zone with possible mineralization, bilobate cells and a "mushroom composite" (mu); (f) recurring structure of veins with attached fusoid cells, most with silica deposition.

**Table 3**. Abundance estimates of the most recurrent phytolith types in the different study locations. Values are percentages (%) of studied leaf samples in a location.

| Location | Theme | Bulli-form | Bilob./ Saddle | Rondel | Long cell | Elong. grass | Prickl. hair | Mush-room | Fusoid cell |
|---|---|---|---|---|---|---|---|---|---|
| San Carlos | absent | 12 | 9 | 91 | 56 | 100 | 62 | 100 | 22 |
| | rare | 28 | 16 | 3 | 19 | 0 | 9 | 0 | 13 |
| | common | 34 | 69 | 6 | 25 | 0 | 25 | 0 | 47 |
| | abundant | 25 | 6 | 0 | 0 | 0 | 3 | 0 | 19 |
| Ojeayo | absent | 12 | 69 | 88 | 77 | 100 | 50 | 100 | 31 |
| | rare | 15 | 0 | 12 | 19 | 0 | 31 | 0 | 23 |
| | common | 50 | 15 | 0 | 4 | 0 | 12 | 0 | 42 |
| | abundant | 23 | 15 | 0 | 0 | 0 | 8 | 0 | 4 |
| Cumarillo | absent | 12 | 0 | 85 | 37 | 100 | 32 | 95 | 20 |
| | rare | 46 | 10 | 12 | 29 | 0 | 22 | 2 | 27 |
| | common | 39 | 90 | 2 | 34 | 0 | 37 | 2 | 37 |
| | abundant | 2 | 0 | 0 | 0 | 0 | 10 | 0 | 17 |
| Tahuamanu | absent | 16 | 3 | 92 | 66 | 89 | 29 | 97 | 21 |
| | rare | 21 | 8 | 8 | 18 | 11 | 5 | 0 | 32 |
| | common | 39 | 68 | 0 | 16 | 0 | 42 | 3 | 39 |
| | abundant | 24 | 21 | 0 | 0 | 0 | 24 | 0 | 8 |
| Primavera | absent | 19 | 0 | 100 | 42 | 92 | 67 | 89 | 6 |
| | rare | 39 | 3 | 0 | 19 | 8 | 22 | 0 | 14 |
| | common | 33 | 86 | 0 | 36 | 0 | 8 | 8 | 50 |
| | abundant | 8 | 11 | 0 | 3 | 0 | 3 | 3 | 31 |
| Chico | absent | 10 | 10 | 100 | 100 | 30 | 70 | 90 | 10 |
| Mendes | rare | 0 | 0 | 0 | 0 | 40 | 20 | 10 | 30 |
| | common | 70 | 80 | 0 | 0 | 30 | 10 | 0 | 10 |
| | abundant | 20 | 10 | 0 | 0 | 0 | 0 | 0 | 50 |
| Maciopira | absent | 14 | 0 | 100 | 100 | 14 | 57 | 57 | 0 |
| | rare | 43 | 0 | 0 | 0 | 86 | 43 | 43 | 14 |
| | common | 14 | 100 | 0 | 0 | 0 | 0 | 0 | 86 |
| | abundant | 29 | 0 | 0 | 0 | 0 | 0 | 0 | 0 |
| Edmilson | absent | 55 | 9 | 100 | 100 | 55 | 45 | 91 | 18 |
| | rare | 36 | 0 | 0 | 0 | 36 | 36 | 9 | 9 |
| | common | 9 | 45 | 0 | 0 | 9 | 9 | 0 | 64 |
| | abundant | 0 | 45 | 0 | 0 | 0 | 9 | 0 | 9 |
| São Tomé | absent | 0 | 0 | 90 | 100 | 100 | 0 | 100 | 20 |
| | rare | 60 | 0 | 10 | 0 | 0 | 20 | 0 | 0 |
| | common | 10 | 70 | 0 | 0 | 0 | 50 | 0 | 60 |
| | abundant | 30 | 30 | 0 | 0 | 0 | 30 | 0 | 20 |
| Campo Alegre | absent | 0 | 0 | 100 | 80 | 40 | 0 | 100 | 10 |
| | rare | 30 | 0 | 0 | 0 | 30 | 40 | 0 | 10 |
| | common | 30 | 80 | 0 | 20 | 30 | 20 | 0 | 40 |
| | abundant | 40 | 20 | 0 | 0 | 0 | 40 | 0 | 40 |
| Ivo | absent | 0 | 0 | 100 | 100 | 100 | 0 | 100 | 0 |
| | rare | 71 | 0 | 0 | 0 | 0 | 0 | 0 | 29 |
| | common | 29 | 57 | 0 | 0 | 0 | 57 | 0 | 43 |
| | abundant | 0 | 43 | 0 | 0 | 0 | 43 | 0 | 29 |

Tomé, Campo Alegre, Ivo) showed some tendency to deviate from the others, but in those three sites relatively few leaves were assessed. In principle, it would be possible to statistically estimate the probability of committing a Type I error in claiming the assemblages are different. However, we believe this estimation would not have been very useful as the photos that represented the leaves were subjectively selected. Additionally, we were not completely satisfied with the classification of the phytoliths. The morphotype classification used in this study was deliberately robust because there was considerable transitional variation in phytolith size, form, surface ornamentation, and internal structure. Pure morphological classification remain puzzling even when applying the international code of phytolith nomenclature (Madella *et al*., 2005). An additional challenge in wet oxidation-based microscopy slides is that the viewing angle can vary because phytoliths can appear in different orientations.

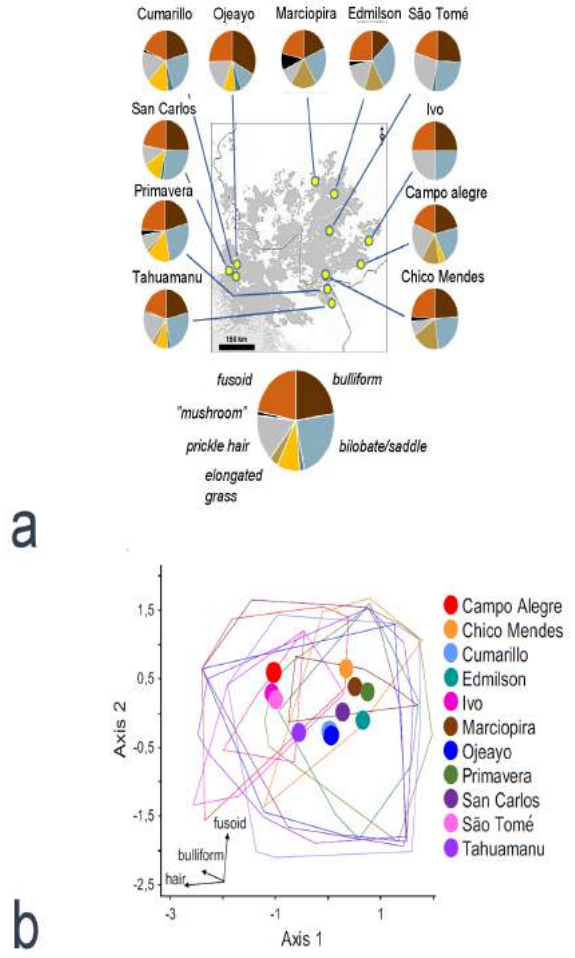


**Fig 7. (a)** Proportions of the most recurrent phytolith morphotypes of the *Guadua* foliar samples in the different locations. The lowermost pie chart shows their proportions in all data and includes a legend for figure colours. (b) Two first axes of a principal components analysis of the spectrum of phytolith morphotypes in 228 *Guadua* leaves. The positions of individual leaves are not shown, but each polygon is drawn as a convex hull around the points representing all leaves of a given site. The points indicate the centre of gravity of the leaves of each site. Colour coding of the polygons and the points is indicated in the legend. The two first axes embrace 51.3% of the total variance. The arrows in the bottom left present the eigenvectors of the three phytolith types that showed the strongest correlations with the two first PCA axes ('fusoid' with correlations of 0.09 and 0.96, and 'hair' of -0.86 and -0.05 with the axes one and two, respectively).

Plant biosilica studies often address morphological characteristics and usefulness in palaeoecological reconstructions and archaeology (Madella *et al*., 2005; Watling *et al*., 2015). The functional role and evolutionary origin of these mineralised grains offer a more dynamic viewing angle (see Dabney III *et al*., 2016). Mineralization promote plant stiffness and can help the plant defend against herbivores and fungal infections (Strömberg *et al*., 2016). In the case of the *Guadua* bamboos, such characteristics could be adaptive and adjustable as suggested by two of our findings. First, the long chains of the large-sized bulliform cells extending deep in the foliar tissue showed different degrees of mineralization. Second, similar variability was found in the fusoid cells, which are typical in bamboos (Metcalfe, 1956; Vega *et al*., 2016; Leandro *et al*., 2018) yet neglected in phytolith literature. It is also questionable whether the mineralized fusoid cells should be considered phytoliths at all. As both of these cell types varied in their degrees of mineralization between different sampling locations, the plain accumulation of silica in aging tissue (Motomura *et al*., 2000) does not seem a plausible explanation. Rather, these findings suggest the bulliform and fusoid cells have an active role in inorganic mineral moving and deposition in *Guadua*. By adjusting the degree of mineralization in these dynamic cells, bamboos may change their physiognomies and thereby adapt to their growing environment. Rising mineralization may help the plant to endure over the annual seasonal drought by keeping the leaves expanded, and the subsequent leaf hardening may help to defend against herbivory. However, the current data does

not allow establishing these connections beyond hypothesizing.

Phytolith-occluded carbon (PhytOC) has been suggested to contribute carbon bio-sequestration from the atmosphere (Parr *et al*., 2010), yet the atmospheric origin of PhytOC is also challenged (Reyerson *et al*., 2016). According to Zuo *et al*., (2014), PhytOC content can be over 0.4% of dry bamboo biomass. In thousand-year-old well-drained soils, PhytOC accounted for up to 82% of the remaining total carbon (Parr and Sullivan, 2005). Considering the vast extension of the Amazonian bamboo forests, these results suggest that *Guadua* phytoliths could play a notable role in the local and regional carbon cycling within Amazonia. However, the proportion of PhytOC in *Guadua* biomass requires further study. Based on earlier studies (Alexandre *et al*., 2015; Dabney III *et al*., 2016), we assume that the dark granule-like internal spots in many of the phytolith morphotypes may correspond to carbon that may be stored in soil.

## Conclusion

*Guadua* bamboos in lowland Amazonia contained about ten recurring foliar phytolith morphotypes, most abundantly bulliform cells, various types of short cells and prickle hairs. Also fusoid cells often showed local mineralization. Comparing the eleven different sampling locations with a span of over 600 kilometres, only minor differences appeared in the overall assembly of the most recurring phytolith morphotypes. In consequence, foliar phytolith assemblies in the *Guadua* bamboo can be construed as considerably consistent.

The proportions of mineralised bulliform cells and fusoid cells varied between the different foliar samples, suggesting their active role in silicon and possibly other mineral movements and deposition. Many of the silica-accumulating cells were found to contain a dark spot inside, which may indicate occluded carbon that might contribute to the sequestration of carbon in bamboo biomass.

## Acknowledgements

We thank prof. D. R . Piperno for encouragement in early stages of this study, and Natalia Reátequi, José de Araujo, Evandro Ferreira, Júlia Gomes da Silva and Júlio Nauan Caruta for cooperation in the field, Arto Peltola and Jukka Manninen for preparing the foliar transverse thin sections, and the Academy of Finland project SUBAMAZON (grant 296406) for funding.

## References

Alexandre, A., Basile-Doelsch, I., Delhaye, T., Borshneck, D., Mazur, J.C., Reyerson, P. and Santos, G.M. 2015. New highlights of phytolith structure and occluded carbon location: 3-D X-ray microscopy and NanoSIMS results. *Biogeosciences* 12(3): 863-873.

Ball, T., Chandler-Ezell, K., Dickau, R., Duncan, N., Hart, T.C., Iriarte, J., Lentfer, C., Logan, A., Lu, H., Madella, M. and Pearsall, D.M. 2016. Phytoliths as a tool for investigations of agricultural origins and dispersals around the world. *Journal of Archaeological Science* 68:32-45.

Dabney, C. III, Ostergaard, J., Watkins, E. and Chen, C. 2016. A novel method to characterize silica bodies in grasses. *Plant Methods* 12(3): 1-10.

de Carvalho, A.L., Nelson, B.W., Bianchini, M.C., Plagnol, D., Kuplich, T.M. and Daly, D.C. 2013. Bamboo-dominated forests of the Southwest Amazon: Detection, spatial extent, life cycle length and flowering waves. *PloS one* 8(1), p.e54852

Leandro, T.D., Rodrigues, T.M., Clark, L.G. and Scatena, V.L. 2018. Fusoid cells in the grass family Poaceae (Poales): A developmental study reveals homologies and suggests new insights into their functional role in young leaves. *Annals of Botany* 122(5): 833-848.

Katz, O., Cabanes, D., Weiner, S., Maeir, A.M., Boaretto, E. and Shahack-Gross, R. 2010. Rapid phytolith extraction for analysis of phytolith concentrations and assemblages during an excavation: An application at Tell es-Safi/Gath, Israel. *Journal of Archaeological Science* 37(7): 1557-1563.

Kurosu, T., Saito, M., and Kikuchi, M. 1973. Observation of thermally induced stress in amorphous

semiconductors by i.r. crossed Nicols. *Solid State Communications*, 12(5), 363-367.

Madella, M., Alexandré, A. and Ball, T. 2005. International code for phytolith nomenclature 1.0. *Annals of Botany* 96(2): 253-260.

McMichael, C.H., Bush, M.B., Silman, M.R., Piperno, D.R., Raczka, M., Lobato, L.C., Zimmerman, M., Hagen, S. and Palace, M. 2013. Historical fire and bamboo dynamics in western Amazonia. *Journal of Biogeography* 40(2): 299-309.

Metcalfe, C.R. 1956. Some thoughts on the structure of bamboo leaves. *Shokubutsugaku Zasshi* 69(820-821):391-400.

Motomura, H., Fujii, T. and Suzuki, M., 2000. Distribution of silicified cells in the leaf-blades of Pleioblastus chino (Franchet et Savatier) Makino (Bambusoideae). *Annals of Botany* 85(6): 751-757.

Nelson, B.W. 1994. Natural forest disturbance and change in the Brazilian Amazon. *Remote Sensing Reviews,* 10(1-3): 105-125.

Olivier, J. and Poncy, O. 2009. A taxonomical revision of *Guadua weberbaueri* Pilg. and *Guadua* sarcocarpa Londoño and PM Peterson (Poaceae). *Candollea* 64(2):171-178.

Parr, J., Sullivan, L., Chen, B., Ye, G. and Zheng, W. 2010. Carbon bio-sequestration within the phytoliths of economic bamboo species. *Global Change Biology* 16(10): 2661-2667.

Parr, J.F. and Sullivan, L.A. 2005. Soil carbon sequestration in phytoliths. *Soil Biology and Biochemistry* 37(1): 117-124.

Piperno, D.R. and Pearsall, D.M. 1998. The silica bodies of tropical American grasses: Morphology, taxonomy, and implications for grass systematics and fossil phytolith identification. *Smithsonian Contributions to Botany* 85:1-40.

Piperno, D.R., 2006. Phytoliths: A comprehensive guide for archaeologists and paleoecologists. Altamira Press, Lanham. 238 p.

Rapp Jr., G. and Mulholland, S.C. eds. 1992. *Phytolith systematics: Emerging issues* (vol. 1). Springer Science & Business Media, New York. 350 p.

Reyerson, P., Alexandre, A., Harutyunyan, A., Corbineau, R., de La Torre, H.M., Badeck, F., Cattivelli, L. and Santos, G. 2016. Unambiguous evidence of old soil carbon in grass biosilica particles. *Biogeosciences*, 13(4):1269-1286.

Strömberg, C.A., Di Stilio, V.S. and Song, Z. 2016. Functions of phytoliths in vascular plants: An evolutionary perspective. *Functional Ecology*, 30(8): 1286-1297.

Twiss, P.C., Suess, E. and Smith, R.M. 1969. Morphological classification of grass Phytoliths 1. *Soil Science Society of America Journal* 33(1):109-115.

Vega, A.S., Castro, M.A. and Guerreiro, C. 2016. Ontogeny of fusoid cells in *Guadua* species (Poaceae, Bambusoideae, Bambuseae): Evidence for transdifferentiation and possible functions. *Flora-Morphology, Distribution, Functional Ecology of Plants* 222: 13-19.

Watling, J., Saunaluoma, S., Pärssinen, M. and Schaan, D., 2015. Subsistence practices among earthwork builders: Phytolith evidence from archaeological sites in the Southwest Amazonian interfluves. *Journal of Archaeological Science: Reports* 4: 541-551.

Watling, J., Iriarte, J., Whitney, B.S., Consuelo, E., Mayle, F., Castro, W., Schaan, D. and Feldpausch, T.R., 2016. Differentiation of neotropical ecosystems by modern soil phytolith assemblages and its implications for palaeoenvironmental and archaeological reconstructions II: Southwestern Amazonian forests. *Review of Palaeobotany and Palynology*, 226, pp.30-43.

Zuo, X., Lu, H. and Gu, Z. 2014. Distribution of soil phytolith-occluded carbon in the Chinese Loess Plateau and its implications for silica–carbon cycles. *Plant and soil*, 374(1-2): 223-232.